2019 IEEE/RSJ International Conference on Intelligent Robots and Systems (IROS)
Macau, China, November 4-8, 2019

Unified Human-Robot Shared Control with Application to Haptic Telemanipulation

Cheong Min Ting Samuel, Keng Peng Tee*

Abstract— **Human-robot shared control (SC) has largely been studied in two complementary forms, namely divisible shared control (DSC) and interactive shared control (ISC). DSC enables clean division of the human and the robot subtasks, thus enabling them to work independently, while ISC allows for flexible intervention to improve the collaborative performance or experience. This paper presents a unified scheme that combines both forms of SCs to attain the benefits of flexibility as well as ease of use when human and robot jointly work on a task together. Based on the idea that flexibility should be embedded in every task constraint that the robot is controlling, we connect ISC into the robot subtask providing a soft boundary between the divided orthogonal subspaces allowing human to access the robot subtask and intervene whenever necessary. We also propose a new simple yet effective Cartesian stiffness adaptation law that enables the robot to modify its endpoint stiffness in the robot's control subspace in the presence of disagreement from the human. Simulations and real robot studies for a teleoperated path-following scenario were performed to demonstrate the flexibility of the unified shared control (USC), which allows the robot to dynamically adapt its task based on the operator's intentions.**

I. Introduction

Research in human-robot shared control seeks to leverage on the complementary proficiencies of human and robot to improve or optimize the collaborative performance (see [1] for a review). Practical applications that benefit from human-robot collaboration include teleoperation [2], [3], coassembly [4], automated driving [5], and rehabilitation [6].

Human-robot shared control (SC) can be categorized into *divisible* and *interactive* schemes, motivated by [7] which introduced the concept of divisible and interactive tasks for human-robot or human-human interactions. Specifically, divisible tasks can be decomposed into component tasks that each partner independently perform, while interactive tasks offer no clear means of subtask division since the actions of one partner significantly affect the performance of the other. In a similar vein, divisible shared control (DSC) distributes the control between the human and the robot so that they are able to control their respective subtasks independent of each other, while interactive shared control (ISC) has overlapping control subspaces and allows for disagreement that drives adaptation in the control to improve the collaborative performance or experience. A similar categorization into *fixed-authority* and *variable-authority* haptic shared control was proposed in [8].

The authors are with the Institute for Infocomm Research, A*STAR, Singapore 138632.
*Corresponding author (E-mail: kptee@i2r.a-star.edu.sg).

For DSC, virtual fixture methods, which constrain motion along certain paths while preventing movement into restricted regions, are popular, especially for surgical assistance and telemanipulation [9]-[13]. A form of DSC for haptic systems was proposed in [14] where the shared controller independently compensated for the internal dynamics of the object so they are transparent to the user when performing a target-hitting task. Besides these, industrial tasks such as welding are also suitable for applying DSC, where the welding robot assists in filtering out user's tremor as the user carefully controls the speed of the welding movement [15]. Our previous work [16] proposed a DSC scheme to assist teleoperation tasks on a curved object surface, with results from the user study suggesting that divisible shared control improves accuracy, speed, and smoothness, while at the same time reduces cognitive load, effort, and frustration.

For ISC, a continuous human-robot role adaptation method was proposed in [17] which adapts the robot's control gain under a game-theoretic framework based on kinesthetic disagreements from the human. This adaptive method was improved in [18] by using neural network based policy iteration to obviate the need for an explicit model of the human dynamics. Other approaches include risk-sensitive optimal control to adaptively switch between model-based and model-free predictions [19] and homotopy-based switching control to dynamically change the roles between leader and follower [20].

As useful as DSC is in actively performing a pre-defined subtask and providing haptic assistance to the user, a disadvantage is its inflexibility in allowing the user to interfere or dynamically redefine the robot's subtask. Any interaction or intrusion in the robot's control subspace is treated as an unwanted conflict and rejected. As a result, the robot is unable to respond to ad-hoc changes in task plans initiated by the human, such as avoiding an obstacle lying on the robot's path.

In this paper, we propose a way to combine DSC and ISC into a unified scheme to achieve the best of both worlds, namely ease of use and flexibility. The key insight is to embed ISC into the robot control subspace divided from the main task, thereby providing a soft boundary between the divided orthogonal subspaces allowing human to access the robot subtask and intervene whenever necessary. Furthermore, we propose a new simple yet effective Cartesian stiffness adaptation law for the embedded interactive shared control, enabling the robot to relax its endpoint stiffness components in the robot's control subspace in the presence of disagreement from the human. In the absence of disagree-

978-1-7281-4004-9/19/$31.00 ©2019 IEEE

ment, the endpoint stiffness smoothly recovers its nominal level. We study the performance of the proposed unified shared control on a telemanipulation application involving moving the robot end effector on a constrained path.

II. Problem Formulation

Consider the task space dynamics of a robot manipulator:

$$M_x(x_r)\ddot{x}_r + C_x(x_r, \dot{x}_r)\dot{x}_r + G_x(x_r) = F_h + \bar{F}_r \tag{1}$$

where x_r, $\dot{x}_r$, $\ddot{x}_r$ denote the robot end effector position, velocity and acceleration respectively, $M_x(x_r)$ the inertia matrix, $C_x(x_r, \dot{x}_r)\dot{x}_r$ the Coriolis and centrifugal forces, $G_x(x_r)$ the gravity forces, and $F_h, \bar{F}_r$ the force inputs attributed to the human and the robot controller respectively.

To compensate for the gravity and Coriolis and centrifugal forces, let

$$\bar{F}_r = C_x(x_r, \dot{x}_r)\dot{x}_r + G_x(x_r) + F_r \tag{2}$$

where F_r is a new input force. This yields the simplified task dynamics:

$$M_x(x_r)\ddot{x}_r = F_h + F_r \tag{3}$$

The control objective of the robot manipulator is two-fold:

1) To ensure that the end effector position $x_r(t)$ tracks a human-specified position $x_h(t)$.
2) To fulfil a set of task constraints in Euclidean space described by $f(x_c) = 0$ (e.g. staying on a path or surface).

These are described as follows:

$$x_r(t) \quad \rightarrow \quad x_h(t) \tag{4}$$

$$x_r(t) \quad \in \quad \Omega_C = \{x_c \in SE(3) \mid f(x_c) = 0\} \tag{5}$$

When both objectives are in consensus, that is, both human and robot share the goal to have the end effector stay on the constraint path ($x_h(t) \in \Omega_C$), divisible shared control along the lines of [16] can be employed to divide the control between the human and the robot such that the human is free to move the end effector along the path while the robot controller constrains the end effector on the path or surface. The control subspaces of the human and the robot are orthogonal, so they control the end effector independently without interfering with each other.

However, when there is disagreement between the objectives, that is,

$$x_h(t) \notin \Omega_C, \quad \text{for some } t \in \Omega_t \subset [0, \infty) \tag{6}$$

divisible shared control no longer suffices to solve the problem, because the task is no longer divisible.

This paper is concerned with solving problem (4)-(5) subject to ad-hoc disagreements:

$$x_h(t) \begin{cases} \notin \Omega_C, & \text{if } t \in \Omega_t \\ \in \Omega_C, & \text{otherwise} \end{cases} \tag{7}$$

An illustrative example is shown in Fig. 1, where initially the human guides the robot end effector to follow a prescribed path, but subsequently tries to deviate it away from the path, due to, for example, an obstacle lying on the path.

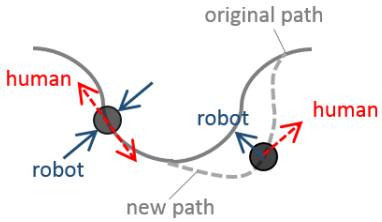

Fig. 1: Human-robot interactive task with path constraint.

III. Unified Shared Control Design

In this section, we propose a unified shared control (USC) framework, combining both divisible and interactive shared control, to solve the human-robot collaboration problem (4)-(5) subject to ad-hoc disagreements from the human (7).

Divisible shared control (DSC), depicted in Fig. 2, involves a main task that can be divided into subtasks controlled separately by the human and the robot, such that they do not interfere with each other.

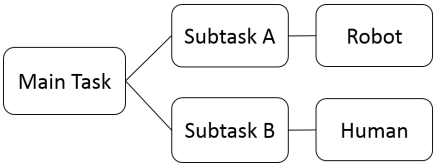

Fig. 2: Divisible Shared Control

For example, in a task of moving on a surface in Euclidean space, a possible divisible shared control scheme [16] decomposes the motion space of the end effector into two complementary subspaces, namely $x_h \in \mathbb{R}^3$ and $\xi_r = (x_r, R_r) \in \mathbb{R}^3 \times SO(3)$, such that

$$x_h \cdot x_r \quad = \quad 0 \tag{8}$$

$$x_h \cup \xi_r \quad \in \quad SE(3) \tag{9}$$

The control of end effector motion in x_h is allocated to the human and ξ_r to the robot controller.

Interactive shared control (ISC), on the other hand, as shown in Fig. 3, does not split the main task, but is instead performed simultaneously by both human and robot. To resolve possible conflict in motion, the robot adapts a set of control parameters K, based on estimated human intention from force or motion measurements, so as to optimize certain performance criteria.

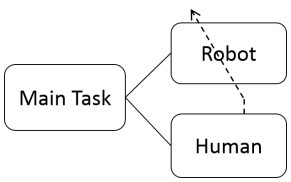

Fig. 3: Interactive Shared Control

For example, in a task where the robot is regulating its end effector position at a point x_r^*, while the human is trying to

pull the end effector to another point, the control forces and control parameter adaptation can be represented by:

$$F_r = -K(x_r - x_r^*) \quad (10)$$
$$\dot{K} = h(K, x_r, x_h) \quad (11)$$

where $h(\cdot)$ is a function that is designed to optimize a given performance criterion.

To combine DSC and ISC, we apply the key insight that flexibility should be embedded in every task constraint that the robot is controlling. Thus, we connect interactive shared control into the robot subtask (Subtask A) as shown in Fig. 4, thereby providing a soft boundary between the divided orthogonal subspaces allowing human to access the robot subtask and intervene whenever necessary. Subtask A, handled by the robot, is allowed to adapt its control to allow for human interaction. The potential of this shared control is to remove the inflexibility from the divisible control to allow for human to interact with the robot's pre-assigned task.

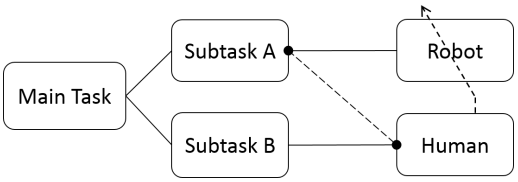

Fig. 4: Unified Shared Control

Under the USC framework, the end effector control forces attributed to the human and robot are designed as follows:

$$F_h = M_x\ddot{x}_h - D_h(\dot{x}_r - \dot{x}_h) - K_p(x_r - x_h) \quad (12)$$
$$F_r = -K_a(t)(x_r - x_c) \quad (13)$$

where K_p and D_h are positive constants, $K_a(t)$ an adaptive gain, and x_c the closest point on the path to the current end-effector position. Based on this constraint position, the restorative force will act to return the end-effector to the path. The further the operator deviates from the path constraint, the higher the restorative force that will be acting on the end-effector.

The adaptive gain K_a represents the controlled stiffness of the end effector with respect to the constraint path. This stiffness can be adjusted to control how much robot assisted control would be applied and also how much robot would allow the human operator to interfere with the its sub-task when required to deviate from the path. The adaptation law for K_a is as follows:

$$\dot{K_a}(t) = -\gamma(K_a(t) - \overline{K}_a) - \lambda D_u \quad (14)$$
$$D_u = \begin{cases} F_u - F_{thres} & \text{, if } F_u > F_{thres} \\ 0 & \text{, otherwise} \end{cases} \quad (15)$$
$$F_u = K_u\|x_r - x_c\| \quad (16)$$

where $K_a(0) = \overline{K}_a$, γ is the gain for the restorative term, λ is the gain for the decay term, K_u is the user gain, $\overline{K}_a$ is the initial norm value for the adaptive gain K_a, and D_u is difference between the user force F_u and the force threshold F_{thres}. A lower bound is imposed on K_a so that it is always non-negative.

As the restorative force is proportional to the adaptive gain, when the adaptive gain is large, the restorative force would also be large enough to effectively overcome the command force and thus, keeps the end-effector within its path constraint. This would indicate that the gain for K_a needs to be significantly larger than K_p. Vice versa, when the adaptive gain is reduced, the operator's induced command force would instead be larger and allows the operator to take control.

When the operator apply a force F_u that is greater than a predefined force threshold F_{thres}, this would signal the robot that the operator wishes to take over control, and hence reduces the restorative force. This allows the command force to eventually take over control when the adaptive gain gets significantly reduced. Conversely, when the operator's control returns and re-approaches the path, the adaptive gain would increase and be re-applied to return the robot's end-effector back to its task.

To analyze the stability, we substitute the end effector control forces (12)-(13) into the task space robot dynamics (3), yielding the closed loop dynamics:

$$M_x\ddot{e}_h + D_h\dot{e}_h + (K_a + K_p)e_h = -K_a(x_h - x_c) \quad (17)$$

where $e_h := x_r - x_h$. By viewing the right hand side as a disturbance to the stable system

$$M_x\ddot{e}_h + D_h\dot{e}_h + (K_a + K_p)e_h = 0 \quad (18)$$

we know that when $\|x_h - x_c\| \to 0$, we have that $e_h \to 0$, that is, $x_r \to x_h$, and $x_r \to x_c$. In other words, when there is consensus between human and robot to follow the path, the robot end effector will converge to and remain in a neighbourhood of the path.

On the other hand, when the human intends to deviate from the path, we have $\|x_h - x_c\| \gg 0$, resulting in $\|x_r - x_c\|$ increasing, eventually triggering the adaptation (14) that decreases K_a to a small value such that the right hand side of (17) is small. This leads to $x_r \to x_h$ again. Therefore, the proposed unified shared control (12), (13) (14)-(16) fulfils task (4)-(5) subject to ad-hoc disagreements (7).

IV. Application in Haptic Telemanipulation

We applied the proposed USC method on a haptic telemanipulation application, where a human operator teleoperated a robotic end effector to move along a path. Such a task is difficult for a human due to impoverished perception of the remote scene. First, simulation was carried out to determine suitable parameter values for stiffness adaptation (14) in USC. Then, comparison of performance between DSC and the proposed USC was studied on a real robot (Fig. 7). For ISC, without the division of subtasks from the DSC, the robot is unaware of the path constraint. Thus, comparison of USC and ISC is omitted in this paper, which only focuses on the path following task.

We considered a sinusoidal path on a horizontal plane. The task was divided into two subtasks, where the robot's

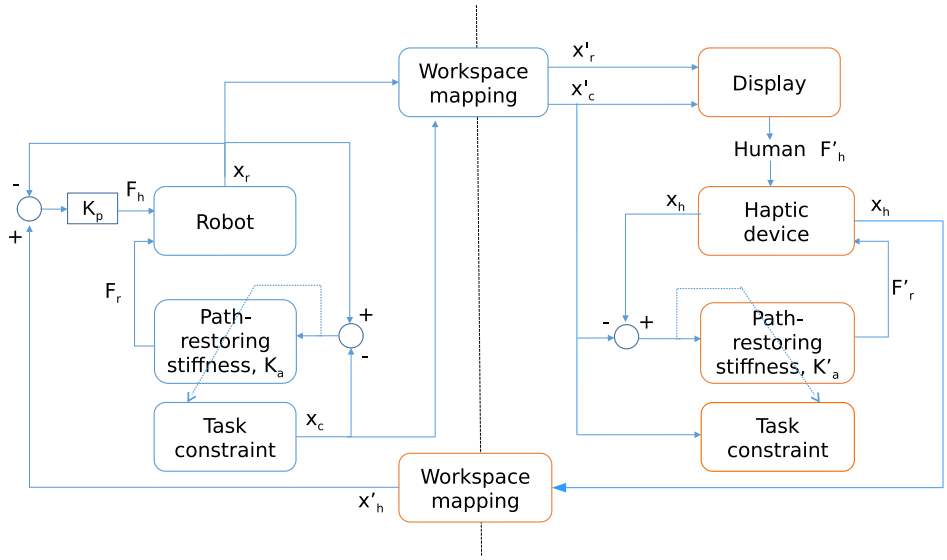

Fig. 5: Haptic telemanipulation scheme

task was to provide restoring forces along the path normal, whereas the human operator was free to move the end effector along the path tangent.

The haptic telemanipulation scheme is illustrated in Fig. 5. As the human operator and robot work in different coordinate frames, mapping was performed between the workspaces. The task constraint, in the form of a designated path, was mapped from the robot workspace to the human operator workspace, i.e. $x_h \rightarrow x'_h$, $x_c \rightarrow x'_c$, $x_r \rightarrow x'_r$. Hence, the path constraint was mirrored at the human operator end, and provided the human operator with similar but scaled-down restoration forces and stiffness. This allowed the human operator to be able to experience the similar force constraint acting on the robot. Assuming that the human operator moves slowly ($\dot{x}'_h$, $\ddot{x}'_h \simeq 0$), we implement, from (12), a simplified form for the end effector control force attributed to the human, $F_h = -K_p(x_r - x'_h)$.

The operator's desired position at a given time, x_h was measured using the Omega.7 haptic device and mapped from the human operator workspace to the robot workspace. Similarly, the robot actual end-effector position x_r was also mapped from the robot workspace to the human operator workspace, and displayed to the operator.

A. Simulation Study

Simulation of the USC was performed in Robot Operating System (ROS) Gazebo to study characteristics of the stiffness adaptation when the operator deviates from and rejoins the 2D path, and to determine suitable values of γ and λ from (14). The adaptation of stiffness K_a with varying λ and γ can be observed in Fig. 6. For ease of comparison, we used a pre-recorded human operator trajectory of deviating and rejoining the path when generating this figure.

The λ term determines the decay rate of the stiffness, i.e. the rate at which the robot hands over control to the operator

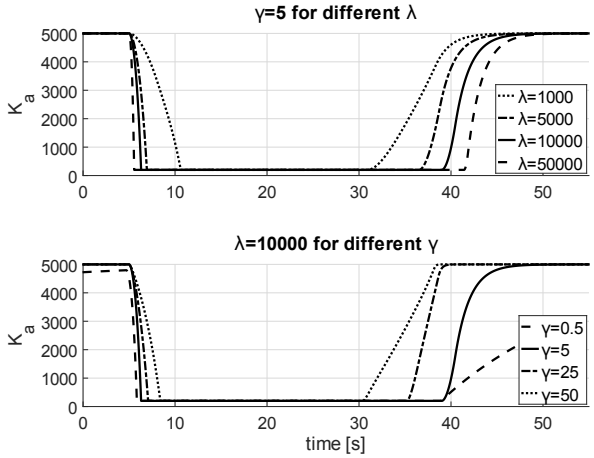

Fig. 6: Characteristics plot of K_a with varying λ (top) and γ (bottom).

when he/she intervenes with the robot's sub-task. Thus, we see that increasing λ increases the rate of stiffness decay. If λ is too small, the operator would find it very difficult to deviate from the path. If λ is too large, the transition can be abrupt and jerky. A good choice of value for λ would be one that is responsive and yet provides sufficiently smooth transition. On the other hand, γ determines the restorative rate of the stiffness, which affects how quickly the robot regains functionality of its subtask after intervention from the operator. An increase in γ would restore the stiffness K_a faster. The ideal transition for the restoration is to be gentle so the operator does not experience a large force feedback from haptic device during the restoration of the robot's subtask. We found that $\gamma = 5$ and $\lambda = 10000$ allow the transition between control states to be smooth and fast.

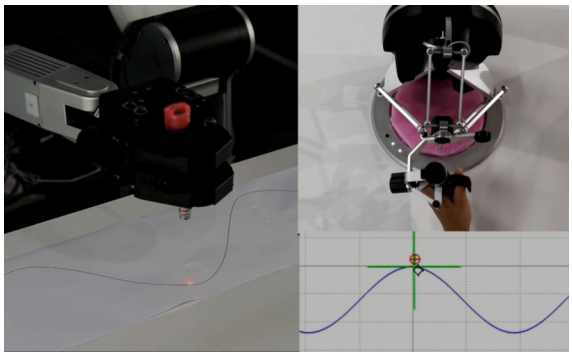

Fig. 7: *Left*: Robotic arm and 2D path-following task. *Upper right*: Omega.7 haptic device for teleoperation. *Bottom right*: Visual display for human operator.

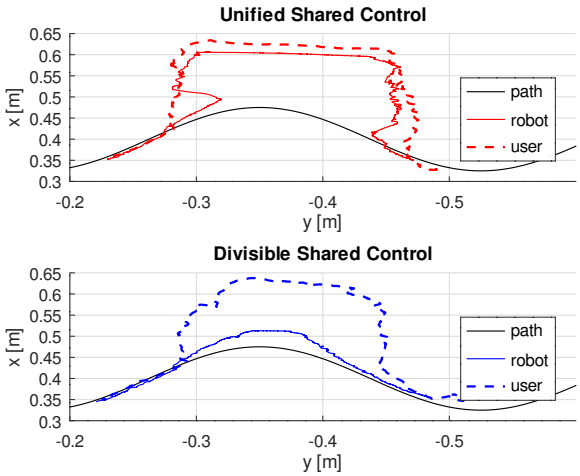

Fig. 8: End-effector position during intentional deviation from original path by human, for unified shared control (top) and divisible shared control (bottom).

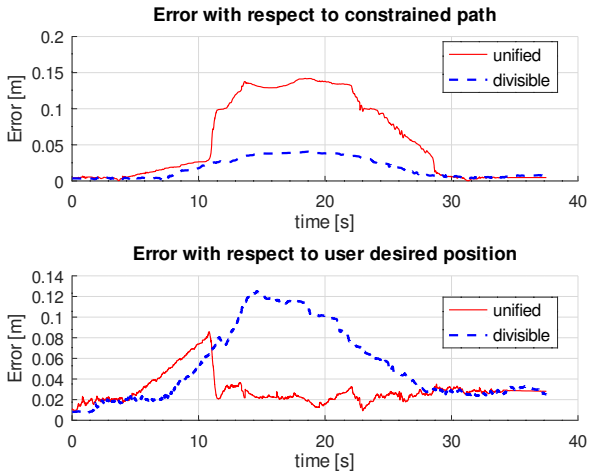

Fig. 9: End-effector position error with respect to constraint path (top) and operator's intended trajectory (bottom).

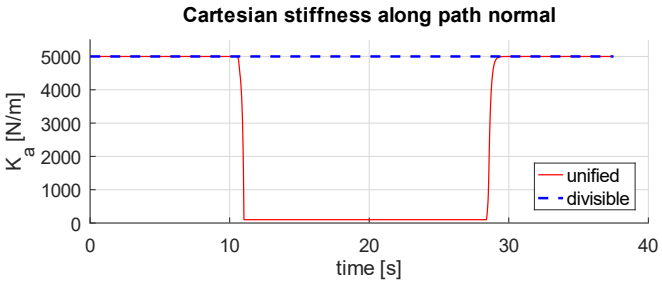

Fig. 10: Restorative stiffness K_a adapts in response to ad-hoc disagreement from the human, with unified shared control.

B. Real Robot Study

In the real robot study, we compared the proposed USC with a DSC on the same 2D path-following task. The following parameters were used: $K_p = 1200$ N/m, $\overline{K}_a = 5000$ N/m, $K_u = 300$ N/m, $F_{thres} = 8$ N, $\gamma = 5$, $\lambda = 10000$.

1) End-effector Position: The actual end effector trajectory and the operator's intended trajectory, both going from left to right, can be seen in Fig. 8. The robot controller was applying forces along the path normal to keep the end-effector on the designated path, while the operator was controlling the end effector to move along the path tangent, where there was no resistance from the robot controller. Corresponding positional errors with respect to the path and the operator's intended trajectory are shown in Fig 9, where we see that DSC has a minimal amount of deviation from the designated path ($<$ 4cm). This was partly because of the round-off error from the mapping of quantities between the operator and robot workspaces, and partly the robot controller allowing a tolerance of ± 5 mm from the path before applying the path-restoring force. This error margin can be reduced by using a larger K_a to K_p ratio. For DSC, the operator managed to stay close to the path with the assistance of the robot controller. However, when the operator wishes to deviate, it could be seen that even when there was a large error from the operator's intended trajectory, the robot did not follow the operator's desired path. This shows the inherent inflexibility of DSC, which ignores any conflict between the operator's intended trajectory and the robot's subtask.

On the other hand, the proposed USC includes additional ability of the ISC to allow for human interaction with the robot's subtask. Initially, the robot was attempting to keep the end-effector within the designated path. However, the increasing error from the path kept eventually caused the force threshold F_{thres} to be exceeded, triggering the robot to quickly and smoothly relinquish control to the operator, and follow the operator's intended trajectory instead of staying on the path. We see this transition when $t = 10$-12s, where the error with respect to the operator's intended position was quickly reduced to around 2.5cm. Conversely, the error from the designated path, increased, due to conflict resolution.

When the operator rejoined the designated path (i.e. no more conflict), the robot regained its subtask control, providing haptic assistance to keep the operator on path smoothly. This can be observed from $t = 28$ s onwards, where both error from the path and error from the operator's intended trajectory are similarly low for DSC and USC.

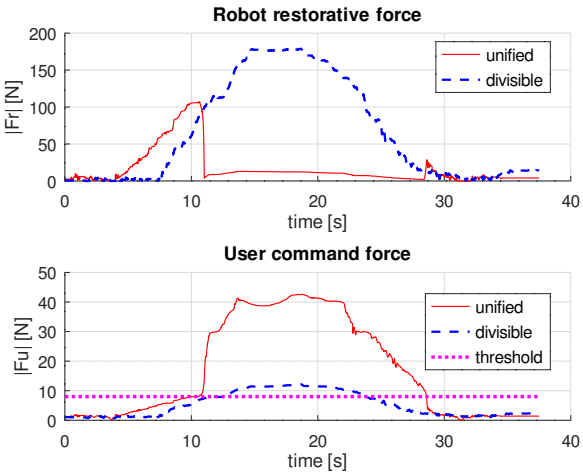

Fig. 11: Restorative force drops sharply when user command force crosses the threshold, with unified shared control.

2) Stiffness Adaptation K_a: For the proposed USC, based on (14), the stiffness K_a reduced sharply to nearly zero (Fig. 10) when the user command force F_u exceeded F_{thres} (Fig. 11) during $t =$ 10-12 s. Subsequently, during $t =$ 12-28 s the operator assumed control and the path-restoring force from the robot controller became very small despite large path deviation. Upon re-entry to the path at $t = 28$s onwards, the user command force F_u dropped below F_{thres}, so K_a was restored to $\overline{K}_a$ (Fig. 10), and a restorative force was immediately applied by the robot controller to return the end-effector to the designated path, as seen by the small spike in the restorative force in Fig.11 during $t =$ 28-30 s.

In the case of DSC, stiffness K_a remained at a high constant value, as seen in Fig. 10. The restorative force reached a high value of 175 N to counteract the operator's attempt to deviate from the designated path. The operator also experienced a scaled-down but large restorative force on the haptic device, which prevents further deviation. Whenever there was conflict between the robot subtask and operator's intention, it resulted in the domination by the restorative force, due to the larger K_a to K_p ratio. Thus, DSC is unable to take into account the intentions of the operator to deviate from the path, unlike the USC.

V. Conclusion

In this paper, we have proposed a unified shared control method which involves the unification of the divisible shared control method with the interactive shared control method to enable greater ease of use and flexibility during human-robot collaborative tasks such as telemanipulation. Simulation and real robot studies have demonstrated that the unified shared control method is able to dynamically adapt to the operator's intention effectively and with a smooth transition, thus allowing for more flexibility in control while performing telemanipulation using a haptic device.

Acknowledgements

We are grateful to Ng Kam Pheng for software development assistance, and Pang Chun Ho and Tan Chong Boon for technical assistance during the robot experiments.

References

[1] S. Musić and S. Hirche, "Control sharing in human-robot team interaction," *Annual Reviews in Control*, vol. 44, pp. 342–354, 2017.
[2] S. Hirche and M. Buss, "Human-oriented control for haptic teleoperation," *Proceedings of the IEEE*, vol. 100, no. 3, pp. 623–647, 2012.
[3] C. Passenberg, A. Peer, and M. Buss, "A survey of environment-, operator-, and task-adapted controllers for teleoperation systems," *Mechatronics*, vol. 20, no. 7, pp. 787 – 801, 2010.
[4] A. Cherubini, R. Passama, A. Crosnier, A. Lasnier, and P. Fraisse, "Collaborative manufacturing with physical humanrobot interaction," *Robotics and Computer-Integrated Manufacturing*, vol. 40, pp. 1 – 13, 2016.
[5] R. Li, Y. Li, S. E. Li, E. Burdet, and B. Cheng, "Driver-automation indirect shared control of highly automated vehicles with intention-aware authority transition," in *2017 IEEE Intelligent Vehicles Symposium (IV)*, 2017, pp. 26–32.
[6] E. Burdet, Y. Li, S. Kager, K. Chua, A. Hussain, and D. Campolo, "Chapter 10 - interactive robot assistance for upper-limb training," in *Rehabilitation Robotics*, R. Colombo and V. Sanguineti, Eds. Academic Press, 2018, pp. 137 – 148.
[7] N. Jarrasse, T. Charalambous, and E. Burdet, "A framework to describe, analyze and generate interactive motor behaviors," *PLoS ONE*, vol. 7, no. 11, p. e49945, 2013.
[8] D. A. Abbink, M. Mulder, and E. R. Boer, "Haptic shared control: smoothly shifting control authority?" *Cognition, Technology & Work*, vol. 14, no. 1, pp. 19–28, 2012.
[9] L. B. Rosenberg, "Virtual fixtures: perceptual tools for telerobotic manipulation," *Proceedings of IEEE annual virtual reality international symposium*, pp. 76–82, 1993.
[10] D. Aarno, S. Ekvall, and D. Kragic, "Adaptive virtual fixtures for machine-assisted teleoperation tasks," in *Proceedings of the 2005 IEEE International Conference on Robotics and Automation*, 2005, pp. 897–903.
[11] M. Li, M. Ishii, and R. H. Taylor, "Spatial motion constraints using virtual fixtures generated by anatomy," *IEEE Transactions on Robotics*, vol. 23, no. 1, pp. 4–19, 2007.
[12] K. Sreekanth, D. Mohan, H. Bo, and D. Campolo, "Manual guidance of a compliant manipulator during curve-following tasks: Basic framework and preliminary experimental tests," in *IEEE Region 10 Conference (TENCON)*, 2016, pp. 3534–3537.
[13] J. Abbott, P. Marayong, and A. Okamura, "Haptic virtual fixtures for robot-assisted manipulation," in *Thrun S., Brooks R., Durrant-Whyte H. (eds) Robotics Research. Springer Tracts in Advanced Robotics*, vol. 28. Berlin, Heidelberg: Springer, 2007, pp. 49–64.
[14] M. K. O'Malley, A. Gupta, M. Gen, and Y. Li, "Shared control in haptic systems for performance enhancement and training," *Journal of Dynamic Systems, Measurement, and Control*, vol. 128, pp. 75–85, 2006.
[15] M. S. Erden and B. Maric, "Assisting manual welding with robot," *Robotics and Computer-Integrated Manufacturing*, vol. 27, no. 4, pp. 818–828, 2011.
[16] K. P. Tee and Y. Wu, "Experimental evaluation of divisible human-robot shared control for teleoperation assistance," in *IEEE Region 10 Conference (TENCON)*, 2018, pp. 182–187.
[17] Y. Li, K. P. Tee, W. L. Chan, R. Yan, Y. Chua, and D. K. Limbu, "Continuous role adaptation for human-robot shared control," *IEEE Transactions on Robotics*, vol. 31, no. 3, pp. 672–681, 2015.
[18] Y. Li, K. P. Tee, R. Yan, W. L. Chan, and Y. Wu, "A framework of human-robot coordination based on game theory and policy iteration," *IEEE Transactions on Robotics*, vol. 32, no. 6, pp. 1408–1418, 2016.
[19] J. R. Medina, M. Lawitzky, A. Molin, and S. Hirche, "Dynamic strategy selection for physical robotic assistance in partially known tasks," in *2013 IEEE International Conference on Robotics and Automation*, 2013, pp. 1180–1186.
[20] P. Evrard and A. Kheddar, "Homotopy-based controller for physical human-robot interaction," in *RO-MAN 2009 - The 18th IEEE International Symposium on Robot and Human Interactive Communication*, 2009, pp. 1–6.